

Molecular-dynamics study of single-atom radiation damage in diamond

W. Wu

Department of Physics, University of Michigan, Ann Arbor, Michigan 48109-1120

S. Fahy*

Department of Physics, University of Michigan, Ann Arbor, Michigan 48109-1120

and Department of Physics, University College, Cork, Ireland[†]

(Received 11 June 1993)

We have modeled single-atom radiation damage events in diamond by a molecular-dynamics simulation, using an empirical interatomic potential to describe the interaction between the atoms in diamond. We find that the damage threshold energy needed to displace a single atom is well above simple estimates based on the diamond cohesive energy. The threshold derived from our simulations is approximately 50 eV, and is relatively insensitive to the direction of initial motion of the displaced atom. The high threshold energy is due to a rapid dissipation of kinetic energy from the bombarded atom into incoherent vibrational energy of its neighboring atoms before the displaced atom can overcome the structural energy barrier to defect formation. This rapid dissipation can be understood qualitatively by noting that when the kinetic energy of a carbon atom is comparable to the damage threshold energy, its velocity is comparable to the speed of sound in diamond.

I. INTRODUCTION

Diamond has long been of technological interest¹ not only for its mechanical properties, but also for its optical and electrical properties (it is transparent over a wide range of frequencies and has high electron mobility when used as a semiconductor). More recently, the development of chemical vapor deposition (CVD) techniques,² which can successfully grow substantial quantities of diamond in thin-film form, has resulted in a resurgence of interest in the general properties of diamond. One of the notable and useful properties of diamond is its radiation hardness, i.e., its resistance to damage of the lattice structure by various forms of high-energy radiation.

The electrical and optical properties of diamond are strongly affected by the presence of defects in the ideal crystal structure. At any finite temperature, entropy considerations demand that there must be a certain thermodynamic equilibrium concentration of defects in the crystal. More important, however, are those defects that are introduced either during the growth of the diamond or during its subsequent processing or use and which are usually not in thermodynamic equilibrium. A defect created in the crystal by a single high-energy radiation event may be frozen in because the energy of thermal fluctuation is too low to anneal the crystal back to its original perfect lattice ordering.

A potentially important application of diamond is its use in high-energy radiation detectors. The first use of diamond in this way was by Woolridge, Ahearn, and Burton³ in 1948. In principle, diamond has many desirable properties for such detectors:⁴ high electron mobility and high electrical breakdown threshold, as well as its resistance to damage by radiation, compared to the more standard silicon or germanium detectors. In the past, practical considerations, such as high cost and concentration of unwanted impurities of natural diamond, have

limited the utility of the material for radiation detectors. However, with the advent of CVD diamond growth,² the possibility of widespread use of diamond in radiation detectors has emerged. Moreover, because of their high radiation damage threshold of diamond, it has been proposed for use as a semiconductor in high-radiation environments, such as in the upper atmosphere and outer space. It is clear that a better understanding of the process of radiation damage is very important to this technology.

There is a wealth of experimental data available for the damage effects of various forms of radiation on diamond.⁵ However, there has been little detailed microscopic theoretical work, apart from an early, very approximate study of Corbett, Bourgoin, and Weigel.⁶ Recent advances in the power of computers and in the development of carbon interatomic potentials have now made detailed microscopic studies of radiation damage processes possible.

The initial event in the damaging of a perfect crystal by radiation is a sudden transfer of a large amount of kinetic energy to the lattice—either to a single atom or many atoms. If their kinetic energy is sufficiently large, the excited atoms then move from their lattice positions, leaving vacancies behind and displacing other atoms from their lattice sites, thus creating a damaged region.

In the present study, we will focus on one aspect of this process, viz., the kinetic-energy threshold required to permanently displace a single atom from its ideal diamond lattice position when all other atoms are initially at rest. In some sense, this may be considered the primary and simplest of all radiation damage events. Despite its fundamental character, the processes involved in this simple damage event have not been previously investigated from a detailed microscopic point of view.

In the simulations presented here, the interaction of the incident high-energy radiation with the diamond lat-

tice will be simulated as a sudden localized input of kinetic energy to one atom. Thus we neglect the subsequent interaction of the radiation particle with the diamond lattice. It corresponds to the situation where the particle is passing through the region of the crystal being studied, but has not yet slowed down enough to actually stop there. This is an appropriate approximation for radiation damage by high-energy electrons (with energies of the order of 1 MeV) or medium-energy neutrons (with energies of the order of 1 keV), where the electrons or neutrons remains energetic after the initial or subsequent collisions. For processes such as ion bombardment or implantation, while our simulations will give some important qualitative insights concerning the transfer of localized energy into the lattice, they cannot accurately represent the damage to the lattice by heavy ions (nitrogen, etc.), where the heavy ion loses much of its energy after the initial collision, and the subsequent interaction and chemical bonding between it and diamond lattice is important.

We will use Tersoff's interatomic potential^{7,8} to calculate the forces between carbon atoms in our molecular-dynamics simulations. The Tersoff potential folds into a classical description of the atoms the known chemical bonding of carbon in the form of bond-stretching, bond-bending, and bond-breaking energies. It is applicable not only to the diamond structure, but also to a wide range of carbon structures far away from the diamond structure.^{7,8} The Tersoff model is sufficiently short ranged (no forces are directly affected by atoms further than 2.1 Å away) that forces can be computed relatively quickly. Once the forces on each atom are determined, Newton's equations of motion can be numerically integrated very accurately using the so-called "leap-frog" method for molecular dynamics,^{9,10} which is accurate to second order in the integration time-step length.

The experimental estimates of the threshold energy for displacing an atom in diamond, derived from high-energy electron scattering, vary from 35 to 80 eV.¹¹⁻¹⁴ A theoretical estimate of 24-30 eV is obtained¹² following the procedure introduced by Kohn¹⁵ for semiconductor defects (where the energy threshold is taken to be the energy to break four bonds plus the work required for the displaced atom to pass through the saddle point and go to an interstitial position). From our simulations, we find that the threshold kinetic energy at 0 K is 47 eV for initial motion of the displaced atom in the $\langle 100 \rangle$ direction, 50 eV in the $\langle 110 \rangle$ direction, and 54 eV in the $\langle 111 \rangle$ direction. As we shall see below, the discrepancy between the estimate obtained following the procedure of Kohn and the threshold obtained from dynamical simulations is caused primarily by a rapid transfer of kinetic energy from the displaced atom into *vibrational energy* of the lattice. Finite-temperature simulations have also been performed, and the effects of finite temperature (300 K) on the threshold energy are found to be negligible.

II. METHOD

The molecular-dynamics (MD) technique was first used in simulating radiation damage by Gibson *et al.*¹⁰ In the

present simulations, the interatomic forces are calculated using the potential of Tersoff.^{7,8} Since we can simulate only a finite number of atoms (of the order of several hundred), while in a real crystal there are practically an infinite number of atoms, we introduce a viscous damping of the atomic motion at the boundaries of our simulated region to mimic the effect of energy absorption into the infinite lattice in a real crystal.¹⁰ (Alternately, one may view this damping as a way of "impedance matching" the boundary of the simulation region for vibrational waves incident on the boundary in order to eliminate reflections which would not be present in the infinite crystal.)

We enforce fixed boundary conditions (rather than periodic or free boundary conditions) on the simulation region as follows: The molecular-dynamics simulation region (a rectangular parallelepiped, consisting of $n_1 \times n_2 \times n_3$ cubic unit cells of the diamond lattice) is embedded in a surrounding structure whose atoms are fixed in their ideal diamond positions, so that the surface atoms of the simulation region are in an ideal diamond atomic environment and the forces acting on the surface atoms of the simulated region are exactly the same as those on the atoms within the simulated region when the system is at rest. Thus the only extra forces needed on all surface atoms are damping forces which dissipate the absorbed energy. In this fashion, we avoid the spurious relaxation of the surface which would occur with free boundary conditions and the problem of appropriate dissipation of the incident radiation energy which arises with periodic boundary conditions.

A detailed description of the form of Tersoff's potential can be found in Ref. 7. Two sets of parameters have been proposed by Tersoff.^{7,8} In our study, where the primary concern is the creation of defects in the diamond structure, the parameters given in Ref. 8 are more appropriate. As mentioned by Tersoff, this set of parameters is constrained to reproduce the energy of the vacancy in diamond given by Bernholc *et al.*¹⁶ That results in a poorer description of graphite, which is, however, not relevant to our study. A smooth cutoff distance is used, as suggested in Ref. 7, since the smoothness of the potential is important in the MD simulation.

We can best understand the relevant differences of the two sets of parameters for the Tersoff interatomic potential (from Refs. 7 and 8, respectively) by examining the structural energy as a single atom is slowly displaced from equilibrium while the surrounding atoms relax (see Fig. 1), using the two different sets of parameters. The curves shown in Fig. 1 are calculated by constraining the displaced atom to move in 0.1-Å steps along the $\langle 100 \rangle$ direction, letting the structure fully relax about the position of the displaced atom at each step, before proceeding to the next step. (Note that the curve is not perfectly continuous and shows some hysteresis effects due to the presence of multiple local minima of the energy of the structure as the position of the displaced atom is varied near the top of the energy barrier.) The difference between structural energy of the ideal diamond structure (atomic displacement=0) and the energy at the local minimum, where the atomic displacement is approximately 3 Å, corresponding to a vacancy interstitial de-

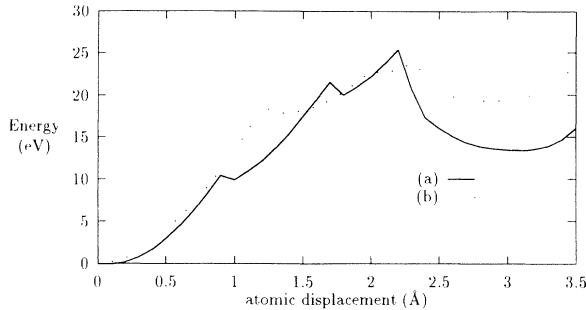


FIG. 1. Potential energy of the relaxed crystal minus the ideal diamond structure energy (in eV) vs atomic displacement (in Å), as one atom is constrained to move along the $\langle 100 \rangle$ direction. The potential energy is calculated for a structure with $6 \times 3 \times 3$ diamond cubic unit-cell structure, with the displaced atom at the center and fixed boundaries. The potential energy was calculated using the Tersoff interatomic potential. Curve *a* was calculated using the parameters for the potential given in Ref. 7 and curve *b* using the parameters in Ref. 8.

fect, gives us an estimate of the defect energies using the two sets of parameters. We see that for the potential from Ref. 7, the peak of the potential barrier at 2.2 Å is 25.4 eV and the local potential minimum at 3.1 Å is 13.4 eV, giving too favorable an energy for the vacancy interstitial defect. For the potential from Ref. 8, the peak of the potential barrier at 2.3 Å is 23.7 eV and the local potential minimum at 2.9 Å is 19.3 eV. For both potentials, the defect structure near the displaced atom is that of the $\langle 100 \rangle$ split interstitial.¹⁷ We will discuss the differences between the two potentials for the dynamical simulations below (see Sec. III).

The viscous damping on the surface atoms cannot perfectly match the effects of the infinite crystal (i.e., no reflection of the energy at the boundary). We seek instead to minimize the reflection of energy at the boundary. This was done by using different values of the damping constant on surface atoms to determine which value gives the maximum dissipation rate of energy out of the simulated region (i.e., the reflection of energy is minimum). Different sizes of structure have been used to check the boundary effects. The results have been found not to be sensitive to boundary effects. The results for a structure with $3 \times 3 \times 3$ cubic unit cells is shown in Fig. 2. The value of the damping constant used in the results presented below was 7×10^{-3} kg/sec.

In all the simulations, we initially give only one atom a velocity along one of the three symmetry axes $\langle 100 \rangle$, $\langle 110 \rangle$, or $\langle 111 \rangle$. This atom which absorbs the initial kinetic energy is chosen to be at the center of the simulation region in order to minimize boundary effects on the results. The size of the simulated region is so chosen that the atoms near the boundaries do not have large displacements from their lattice sites when they finally settle down after the damage event. In this way, we can be sure that the structure is big enough to contain all the damage events and at the same time small enough to be computationally manageable. We have performed simulations for

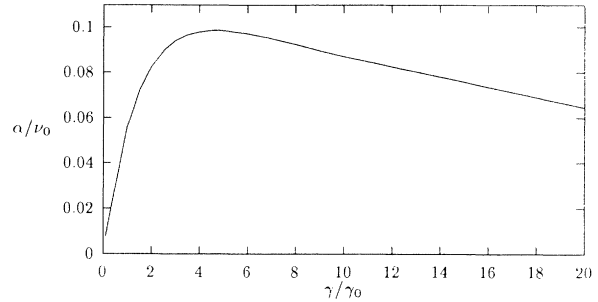


FIG. 2. Energy decay rate α out of the simulated region (in units of the optical-phonon frequency, $\nu_0 = 4 \times 10^{13}$ Hz), as a function of damping constant for surface atoms (in units of $\gamma_0 = 1.56 \times 10^{-3}$ kg/sec). Since most of the energy is lost during the initial stage, we have used the data in the first ten optical-phonon periods in a least-squares fitting of the rate. The curve is based on a $3 \times 3 \times 3$ structure, where 94 atoms are in the simulated region.

regions with $3 \times 3 \times 3$, $4 \times 4 \times 4$, $5 \times 3 \times 3$, $5 \times 5 \times 3$, and $6 \times 3 \times 3$ diamond cubic unit cells. We find only minor changes in the damage thresholds from the smallest to the largest, but find that the structure of the final defects is significantly affected by boundaries in the smallest. (Note that the effects of long-range crystal strain fields on the final defect energies is not accurately included here. However, on the energy scale of interest in this study, this is a very small effect.)

A natural and convenient set of units for discussion for the dynamics in the present problem can be chosen as follows: unit length $L_0 = 1$ Å and unit energy $E_0 = 1$ eV; the unit time $T_0 = 2.502 \times 10^{-14}$ sec is such that a carbon atom with a kinetic energy of 1 eV would have unit velocity $V_0 = 3.994 \times 10^3$ m/sec. We note that the unit of time, T_0 , happens to be very close to the period of the Γ -point optical phonon, which is 2.506×10^{-14} sec, and so provides a convenient time scale for the discussion of localized vibrational processes in the crystal.

For an accurate numerical integration of Newton's equations of motion, the integration step should be chosen so that the forces do not vary abruptly from one step to the next. As might be expected intuitively, we have found that by keeping the integration step to be much smaller than the shortest phonon period, the variations of forces can be kept smooth. In our simulations, at the initial stage of the damage events (for about ten optical-phonon periods), when the velocity of some atoms can be very large, the integration step is $T_0/100 = 2.5 \times 10^{-16}$ sec (i.e., $\frac{1}{100}$ of the optical-phonon period). At a later stage, when the velocities of all atoms are slow, the integration step is chosen to be $T_0/40$. Smaller integration steps have been used in test runs to check the accuracy of integration using these integration step lengths, and we find that the integration steps chosen are sufficiently accurate for our simulation.

The effects of finite temperature in the lattice can be introduced by having random external forces on the boundaries, corresponding to the thermal vibrations of the ex-

tended crystal. The magnitude of the Brownian forces of the surface atoms is chosen to satisfy the fluctuation-dissipation theorem, given the damping of the boundary atoms discussed above. Then the Langevin equation can be integrated and finite-temperature effects can be incorporated into the simulation.¹⁸

III. RESULTS

We have performed simulations for values of the initial kinetic energy of the displaced atom in the range 0–70 eV. We initially give only one atom a velocity along one of the three symmetry axes $\langle 100 \rangle$, $\langle 110 \rangle$, or $\langle 111 \rangle$. (We have also performed some simulations with the initial velocity directed slightly off these high-symmetry directions, without any significant change in the results.) The damage thresholds for initial motion in the major symmetry directions are presented in Table I.

In order to give some idea of the sensitivity of these results to the exact form of the potential used, we show results for the Tersoff potential, using the two different sets of parameters from Refs. 7 and 8. As discussed above, the potential from Ref. 8 is more appropriate for the present purposes. However, the results for the damage thresholds using the two different potentials do not differ greatly, except for the rather high value in the $\langle 111 \rangle$ direction for the potential from Ref. 7.

The most notable aspect of the dynamical simulations is that the damage threshold is approximately twice as large as the energy barrier for adiabatic displacement of the atom. The final defect structure formed is, however, the same as when the atom is adiabatically displaced along the appropriate direction.

The defects along the $\langle 100 \rangle$ and $\langle 111 \rangle$ directions are rather stable and form for a wide range of impulse energies. The defect created along the $\langle 110 \rangle$ direction, on the other hand, is unstable and exists only over a window of approximately 1 eV above threshold; for initial kinetic energies above a second threshold, the broken bonds reform and the displaced atom returns to its original lattice position, leaving the lattice intact. Thus, although the initial damage threshold for displacement in the $\langle 110 \rangle$ direction is close to the thresholds in the $\langle 100 \rangle$ and $\langle 111 \rangle$ directions, no stable defect structure is formed in the $\langle 110 \rangle$ cases and the incipient lattice damage is not

TABLE I. Kinetic-energy threshold for defect formation and the resulting defect energies for various directions of the initial velocity of the displaced atom. Pot. I and Pot. II are the results using the interatomic potentials from Refs. 7 and 8, respectively. (Note that Pot. II is expected to be more accurate potential for the present application.) The size of the structures simulated is (see text) $6 \times 3 \times 3$ for the $\langle 100 \rangle$ direction and $4 \times 4 \times 4$ for the $\langle 110 \rangle$ and $\langle 111 \rangle$ directions. All energies are given in eV. All results are for 0 K.

Direction	Threshold		Defect energy	
	Pot. I	Pot. II	Pot. I	Pot. II
$\langle 100 \rangle$	51	47	13.1	19.5
$\langle 110 \rangle$	52	50	13.5	18.4
$\langle 111 \rangle$	66	54	24.5	24.1

permanent. We have not investigated much higher initial kinetic energies, where more complex defect structures may form.

By examination of the detailed trajectories of the atoms in the simulation, we observe that the presence or absence of permanent lattice damage is clearly resolved soon after the initial impulse to the atom. In Fig. 3 we show the displacement along the $\langle 110 \rangle$ direction of the atom, knocked in that direction from its ideal lattice position, as a function of time elapsed after the initial impulse. We see that, after a large initial displacement, the atom which received an initial kinetic energy of 46 eV (just below threshold) settles back to its original location, without any lattice damage. For an initial kinetic energy of 48 eV (just above threshold), an indication of permanent lattice damage is resolved very soon after the initial impulse, as the displaced atom oscillates about its final defect location.

We have also performed simulations at finite temperature, allowing the lattice to reach thermal equilibrium before and after the application of a large impulse to one of the atoms. The results at 300 K are similar to the results at 0 K. Note, however, that the time scale of our simulations does not allow us to investigate the possibility of slow thermal annealing of the vacancy interstitial pairs formed in the initial damage process.

IV. DISCUSSION

The value obtained for the damage threshold is very close to the most recent value of 55 eV, proposed by Prins, Derry, and Sellschop¹⁴ on the basis of ion bombardment experiments. Prins, Derry, and Sellschop devised a statistical model with the assumption that volume expansion at low ion doses is a direct measure of immobile vacancies remaining in the damaged region after the out-diffusion of interstitials. After obtaining the vacancy-ion number from their experiment, they then compared it with the results from the TRIM program (transport of ions in matter, a Monte Carlo program which follows the collisions each ion undergoes in target

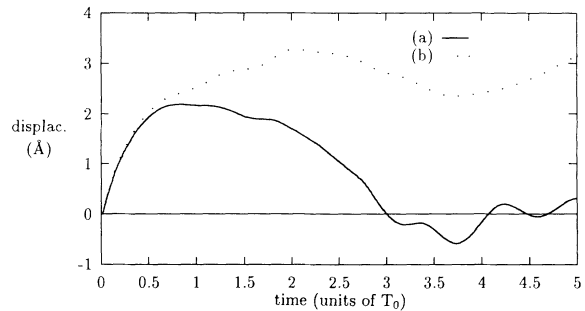


FIG. 3. Displacement of the knocked atom from its lattice position (in Å) along the $\langle 100 \rangle$ direction as a function of time elapsed (in units of the optical-phonon period, 2.5×10^{-14} sec) after the initial impulse. Curve *a* corresponds to an initial kinetic energy of the atom equal to 46 eV (motion along the $\langle 100 \rangle$ direction), which is 1 eV below the damage threshold energy, and curve *b* to an initial kinetic energy of 48 eV, which is 1 eV above the damage threshold.

material).¹⁹ A value of 55 eV for the displacement energy was found to produce the same number of vacancies per ion in the simulations as found experimentally.

The most striking aspect of the dynamical simulations is the fact that the damage threshold proves to be much higher than the energy barrier for "adiabatic formation" of the defect. One might have assumed that, as long as the initial kinetic energy is somewhat greater than the potential energy barrier height in Fig. 1, a defect would be created. Indeed, the height of the barrier for adiabatic displacement of an atom is very close to the threshold energy¹² estimated following the procedure of Kohn.¹⁵ Thus any underestimation of the threshold in Ref. 12 is not due to a poor estimate of the bond-breaking or crystalline strain energies, which give rise to the energy barrier in Fig. 1.

Rather, the large discrepancy is due to the fact that, as the energized atom moves through the diamond lattice, it loses a substantial fraction of its initial kinetic energy, not only to the static local strain energy of the lattice, but to the *vibrational energy* of its surrounding atoms before it can reach the barrier. Thus the atom cannot climb the potential barrier by having "just enough" initial kinetic energy to overcome the adiabatic energy barrier; it must have much more initial energy in order to reach the top of the potential barrier, having irreversibly lost a large fraction to vibrational energy of the lattice (i.e., approximately harmonic, incoherent lattice vibrations) on its way to the top.

This is illustrated in Fig. 4, which shows the evolution of the distribution of kinetic and potential energies among the atoms after an initial impulse of 48 eV in the $\langle 100 \rangle$ direction to the displaced atom. We see that a large fraction of the initial kinetic energy of the displaced atom is transferred to the other atoms in the simulation before it reaches the top of the potential-energy barrier. When the displaced atom has a displacement near the top of the potential shown in Fig. 1 (at a time of $0.67T_0$ in Fig. 4), the kinetic energy of the whole system is approximately 11.3 eV and the potential energy is approximately 36.6 eV.

If we break down these energies at the peak of the energy barrier, assigning an energy to approximately in-

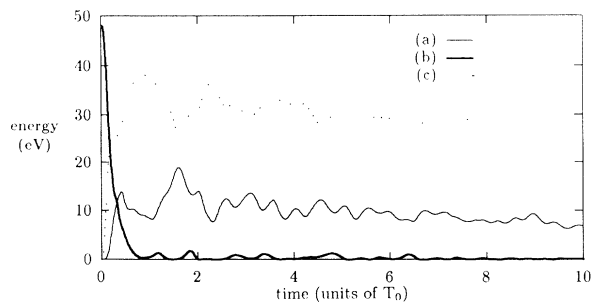


FIG. 4. Kinetic energy of all the atoms except the displaced atom in a $6 \times 3 \times 3$ structure (curve *a*), kinetic energy of the displaced atom (curve *b*), and potential energy of all the atoms (curve *c*), as a function of the time (in units of the optical-phonon period, 2.5×10^{-14} sec) elapsed since bombardment.

coherent harmonic vibrations of the system equal to twice the kinetic energy of atoms other than the displaced atom (since the kinetic and potential energies are equal for incoherent harmonic vibrations), we are left with a remaining contribution of 25.3 eV, which we may assign to a "static" strain energy of the system. Although the pattern of oscillations of the potential and kinetic energies of the total system shortly after passage of the displaced atom over the barrier shows that the vibrational energy of the system is not *completely* incoherent for some time (approximately $2T_0$) after the initial event, nevertheless the energy of the system at time $2T_0$ can be simply viewed as being made up of approximately 19–20 eV of defect formation energy, with an average of 12–13 eV each in the vibrational kinetic and potential energies. Thus the approximate assignment of "static strain" and "incoherent harmonic vibration" energies determined by the time the displaced atom reaches the energy barrier to defect formation remains qualitatively valid for all times afterwards. In this sense, we may think of the loss of kinetic energy of the displaced particle as consisting simply of two components: one to the (reversible) strain energy and the other (irreversible loss) to the incoherent vibrations (or heat) of the lattice. The results of Fig. 4 suggest that this qualitative picture applies even on the very short time scale of initial damage process (time $< T_0$).

We note that the total transfer of kinetic energy from the knocked atom to all other atoms in the finite crystal is slightly higher than that indicated in Fig. 4 since we are only dealing with the atoms in the simulated region and do not account exactly for kinetic energy transferred across its boundary in the infinite crystal. This loss of kinetic energy to the distant atoms of the crystal is represented in our simulations by viscous damping of atoms near the boundary as the initially localized disturbance propagates out to the boundary, which can be seen in Fig. 4 by the slow decay of the total energy of the system.

The time scale for transfer of localized kinetic energy to the vibrational energy of the lattice is determined in a qualitative way by the speed of sound in the crystal. This transfer of energy is not primarily due to anharmonic coupling of the normal modes of the crystal, but occurs because the initial localized motion of a single atom is not a single harmonic mode of the crystal—rather, the initial motion can be considered to be a superposition of crystal normal modes with momenta throughout the Brillouin zone, each of which executes harmonic motion at the appropriate phonon frequency. Even before anharmonic coupling can dephase the initial superposition of normal modes and cause a strictly *incoherent* mixture of modes (i.e., heat), the large range of incommensurate phonon frequencies excited will rapidly give rise to an equal amount of potential and kinetic vibrational energies distributed over many atoms of the system. For the present purposes, this distributed variational motion of the system is indistinguishable from heat.

The vibrational energy will be transported through the system at a speed comparable to the speed of sound, which is given approximately by $\sqrt{B/\rho}$, where B is the

bulk modulus and ρ is the density. For diamond, $\sqrt{B/\rho} \approx 1.1 \times 10^4$ m/sec. (In fact, we find that the highly localized disturbance simulated here propagates somewhat faster than this as a result of dispersion at large momenta in the Brillouin zone, but the qualitative argument remains valid.) However, a carbon atom with a kinetic energy of 25 eV (approximately equal to the potential-energy barrier for adiabatic displacement of an atom) has a velocity of 2×10^4 m/sec, less than twice the speed of sound. With this comparison in mind, it is not then surprising that a substantial fraction of its kinetic energy is transferred to vibrations of the lattice before it can reach the top of the energy barrier shown in Fig. 1.

Although the radiation damage process is not by any means adiabatic, nevertheless the "adiabatically relaxed" potential energy curve in Fig. 1 does appear to have direct relevance for the dynamical behavior. From Fig. 3, we can see that for an initial kinetic energy of 46 eV, 1 eV below the threshold energy, the energized atom moves away from its lattice position by as much as 2.19 Å. But in Fig. 1, the highest point of the potential barrier occurs at 2.3 Å with a value of 23.7 eV. So the knocked atom does not climb over the barrier and it is bounced back from the potential barrier, eventually settling down around its original position without any damage to the lattice. For an initial kinetic energy of 48 eV, we can see from Fig. 3 that the kicked atom successfully passes the top of the potential barrier (where our above assignment of 25.3 eV to a "static strain energy" proves to be remarkably close to the barrier of 23.7 eV from Fig. 1) and settles in a damped oscillatory fashion about a new equilibrium position, finally forming the vacancy interstitial defect.

For atoms moving at the velocities appropriate for single-defect formation (25–70 eV), the qualitative picture which emerges from the simulation is that of the knocked atom passing through a highly viscous medium under the influence of a potential-energy surface deter-

mined approximately by the "relaxed adiabatic" potential energy. It is quite remarkable that this picture applies, even on the short time scale relevant to the initial formation of the simple defects. This qualitative picture of the energy-transfer process (and its associated time scale) should also be relevant to localized dynamical processes involving other bombarding particles, such as in implantation, where chemical bonding changes may also occur.

In conclusion, we have simulated the microscopic process of single-atom displacement due to radiation damage in diamond. We find that the kinetic-energy threshold for permanent lattice damage is approximately 50 eV. This value is in accord with the suggested range of values of Clarke and Mitchell,¹³ derived from experiments using high-energy electron bombardment of diamond. Also, this value is very close to the value of 55 eV more recently proposed by Prins, Derry, and Sellschop¹⁴ for the displacement energy in diamond. We find that the damage threshold is approximately twice as large as the estimate¹² based on the sum of bond-breaking and crystal strain energies. This discrepancy is due primarily to the rapid transfer of kinetic energy from the displaced atom to incoherent vibrations (heat) of the surrounding crystal before the atom can reach the top of the energy barrier for defect formation. The transfer of kinetic energy is effective on the time scale of the present problem because the speed of the displaced carbon atom is comparable to the speed of sound in diamond. Thus the exceptional radiation hardness of diamond is due, not only to its large binding energy, but also to its high sound velocity.

ACKNOWLEDGMENTS

We wish to thank J. Tersoff for useful discussions concerning the parameters in the interatomic potential. Work at the University of Michigan has been supported by the Office of Naval Research under Contract No. N000-14-91-J-1398.

*Electronic address: step8015@bureau.ucc.ie

†Permanent address.

¹*The Properties of Diamond*, edited by J. E. Field (Academic, New York, 1979).

²Recent reviews include J. C. Angus and C. Hayman, *Science* **241**, 913 (1988); W. Yarbrough and R. Messier, *ibid.* **247**, 688 (1990).

³D. Woolridge, A. Ahearn, and J. Burton, *Phys. Rev.* **71**, 913 (1948).

⁴S. F. Kozlov, *IEEE Trans. Nucl. Sci.* **NS-22**, 160 (1975).

⁵For a review, see J. P. E. Sellschop, in Ref. 1, p. 107.

⁶J. W. Corbett, J. Bourgoin, and C. Weigel, in *Radiation Damage and Defects in Semiconductors*, edited by J. E. Whitehouse, IOP Conf. Proc. No. 16 (Institute of Physics, London, 1972), p. 1.

⁷J. Tersoff, *Phys. Rev. B* **37**, 6991 (1988); *Phys. Rev. Lett.* **61**, 2879 (1988); *Phys. Rev. B* **39**, 5566 (1989).

⁸J. Tersoff, *Phys. Rev. Lett.* **64**, 1757 (1990).

⁹S. Duane, A. D. Kennedy, B. J. Pendelton, and D. Roweth, *Phys. Lett. B* **195**, 216 (1987).

¹⁰J. B. Gibson, A. N. Goland, M. Milgram, and G. H. Vineyard,

Phys. Rev. **120**, 1229 (1960).

¹¹C. D. Clark, P. J. Kemmey, and E. W. J. Mitchell, *Discuss. Faraday Soc.* **31**, 96 (1961).

¹²J. C. Bourgoin and B. Massarani, *Phys. Rev. B* **14**, 3690 (1976).

¹³C. D. Clark and E. W. J. Mitchell, in *Radiation Effects in Semiconductors*, edited by N. B. Uriil and J. W. Corbett, IOP Conf. Proc. No. 31 (Institute of Physics and Physical Society, London, 1977), p. 45.

¹⁴J. F. Prins, T. E. Derry, and J. P. F. Sellschop, *Phys. Rev. B* **34**, 8870 (1986).

¹⁵W. Kohn, *Phys. Rev.* **94**, 1409 (1954).

¹⁶J. Bernholc, A. Antonelli, T. M. Del Sole, Y. Bar-Yam, and S. T. Pantelides, *Phys. Rev. Lett.* **61**, 2689 (1988).

¹⁷See, for example, M. Lannoo and J. Bourgoin, *Point Defects in Semiconductors I* (Springer, Berlin, 1981), p. 7.

¹⁸H. Risken, *The Fokker-Planck Equation*, 2nd ed. (Springer, Berlin, 1989), Chap. 3.

¹⁹J. P. Biersack and L. G. Haggermark, *Nucl. Instrum. Methods Phys. Res.* **174**, 257 (1980).